J Comp Physiol A (1993) 173:257–274

Journal of Comparative Physiology A Sensory, Neural, and Behavioral Physiology

Commissural neurons of the electrosensory lateral line lobe of *Apteronotus leptorhynchus*: morphological and physiological characteristics

J. Bastian[1], **J. Courtright**[1], **J. Crawford**[2]

[1] Department of Zoology, University of Oklahoma, Norman, OK 73019, USA
[2] Parmly Hearing Institute, Loyola University, 6525 North Sheridan Road, Chicago, IL 60626, USA

Accepted: 15 May 1993

Abstract. Extracellular injections of horseradish peroxidase were used to label commissural cells connecting the electrosensory lateral line lobes of the weakly electric fish *Apteronotus leptorhynchus*. Multiple commissural pathways exist; a caudal commissure is made up of ovoid cell axons, and polymorphic cells' axons project via a rostral commissure. Intracellular recording and labeling showed that ovoid cells discharge spontaneously at high rates, fire at preferred phases to the electric organ discharge, and respond to increased receptor afferent input with short latency partially adapting excitation. Ovoid cell axons ramify extensively in the rostro-caudal direction but are otherwise restricted to a single ELL subdivision. Polymorphic cells are also spontaneously active, but their firing is unrelated to the electric organ discharge waveform. They respond to increased receptor afferent activity with reduced firing frequency and response latency is long. Electrical stimulation of the commissural axons alters the behavior of pyramidal cells in the contralateral ELL. Basilar pyramidal cells are hyperpolarized and nonbasilar pyramidal cells are depolarized by this type of stimulation. The physiological results indicate that the ovoid cells participate in common mode rejection mechanisms and also suggest that the ELLs may function in a differential mode in which spatially restricted electrosensory stimuli can evoke heightened responses.

Key words: Electric fish – Electroreception – Commissural neurons – Common mode rejection – Sensory processing

Abbreviations: ccELL, caudal commissure of the ELL; CE, contralaterally excited; DML, dorsal molecular layer; ELL, electrosensory lateral line lobe; EOD, electric organ discharge; HRP, horseradish peroxidase; IE, ipsilaterally excited; MTI, mouth-tail inverted; MTN, mouth-tail normal; rcELL, rostral commissure of the ELL; TRI, transverse inverted; TRN, transverse normal

Correspondence to: Joseph Bastian

Introduction

The electrosensory lateral line lobe (ELL) of weakly electric fish is a multilaminar structure which receives the primary electroreceptor afferent projection, massive descending projections from higher-order electrosensory centers, and commissural inputs from the contralateral ELL. The anatomical and physiological studies of this structure have primarily focused on the characteristics of its ascending projection cells and on the roles of its descending afferents in modulating the characteristics of the ELL output neurons (Carr and Maler 1986; Bastian 1986a–c, 1993). This study provides descriptions of the anatomy and physiology of commissural neurons which mediate communication between the ELLs.

The ELL is subdivided mediolaterally into 4 segments, the lateral 3 of which each receives a complete somatotopic projection of the tuberous, or high-frequency, receptor afferents. The 4th, medial segment, receives the ampullary or low-frequency sensitive receptor projection (Heiligenberg and Dye 1982). Each of these subdivisions consists of a ventral fiber layer containing receptor afferents, and in the lateral 3 maps, efferent spherical cells. Dorsal to the fiber layer lies the granule cell layer which contains the inhibitory type I and II granule interneurons. A second fiber layer, the plexiform layer, lies immediately above the granule cell layer and is composed of ELL efferent axons. The layer containing the majority of ELL efferent neurons, the polymorphic layer, is dorsal to the plexiform layer. The dorsal and ventral molecular layers lie above the polymorphic layer and descending inputs from higher-order electrosensory regions terminate within these. The ventral molecular layer receives a direct descending input from the midbrain nucleus praeeminentialis. The dorsal molecular layer is composed of cerebellar-like parallel fibers arising in an overlying mass of granule cells, the posterior eminentia granularis, which also receives descending electrosensory information from the nucleus praeeminentialis as well inputs from proprioceptive nuclei (Carr and Maler 1986

for review; Maler 1979; Maler et al. 1981; Sas and Maler 1983, 1987).

The ELL efferent neurons differ in the types of information that they carry to higher centers. The spherical cells provide the midbrain with precise information about the timing of each cycle of the electric organ discharge (EOD). This information is critically important for the well studied jamming avoidance response, a behavior by which the animals alter their EOD frequency away from the discharge frequencies of conspecifics which might otherwise interfere with the animals' electrolocation abilities (see Heiligenberg 1986, 1991a,b for reviews). The remaining categories of ELL output neurons – the basilar, deep basilar, and nonbasilar pyramidal cells – encode information about the amplitude of the electric organ discharge. The basilar and deep basilar pyramidal cells receive excitatory input directly from electroreceptor afferents and, therefore, respond to increased electroreceptor afferent input with increased firing frequency (E-cells). Nonbasilar pyramidal cells (I-cells) respond to increased EOD amplitude with reduced firing frequency; these are driven by inhibitory interneurons, type I and II granule cells, which receive receptor afferent input (Saunders and Bastian 1984; Bastian and Courtright 1991; Metzner and Heiligenberg 1991; Shumway 1989).

The pyramidal cells and several categories of inhibitory interneurons extend apical dendrites into the overlying molecular layers. Inputs to these molecular layers from higher electrosensory processing regions, principally the n. praeeminentialis, influence the sensitivity or gain of pyramidal cells, shape their temporal response characteristics, and influence the spatial attributes of their receptive fields (Sas and Maler 1983; Bastian 1986a–c, 1993; Bastian and Bratton, 1990; Bratton and Bastian 1990; Shumway and Maler 1989; Shumway 1989).

Three additional ELL efferent neuron types have been shown or suggested to make commissural connections between the ELLs. The polymorphic cells, a relatively heterogeneous category, are found interspersed among the pyramidal cells throughout the polymorphic cell layer, and were shown by Maler et al. (1982) to be retrogradely labeled following HRP injections in the contralateral ELL. The polymorphic cells receive receptor afferent inputs, inputs from inhibitory interneurons, and descending electrosensory information via their apical dendrites. The ovoid and multipolar cells are relatively rare cell types found in the deep fiber layer. They receive receptor afferent input, and in the case of ovoid neurons, this is mediated by both chemical and gap junction inputs (Maler 1979; Maler et al. 1981; Yamamoto et al. 1989). Maler and Mugnaini (1986; personal comm.) have identified the GABAergic elements within the gymnotid electrosensory system. They found a dense plexus of GABAergic fibers within the ELL granule cell layer that is composed of the processes of ELL commissural cells.

This study provides additional anatomical descriptions of the commissural neurons and shows that the polymorphic and ovoid cells project to the contralateral ELL by completely different routes. The intracellular recording and labeling experiments provide preliminary descriptions of the ovoid and polymorphic cell's physiological characteristics and identify the ovoid cells as contributors to the GABAergic fiber plexus found in the ELL granule cell layer.

Methods

The weakly electric fish *Apteronotus leptorhynchus* was used in all experiments. The methods for surgery, extracellular injections of HRP, perfusion, and histological procedures for HRP and Lucifer yellow were the same as described by Bastian and Courtright (1991).

Physiological studies. Animals were suspended in a Plexiglas tank $30 \times 30 \times 7$ cm deep and artificially respirated with a continuous flow of aerated water delivered via a tube inserted into the mouth. Water temperature ranged from 25 to 28°C and conductivity was maintained at 10 kΩ · cm. Intracellular recordings were made with micropipettes filled with either 10% HRP in 1 *M* KCl plus 0.01 *M* Tris adjusted to pH 7.4, or 10% Lucifer yellow CH (Sigma) dissolved in 0.1 *M* LiCl, or with 3 *M* potassium acetate. If electrode resistance was greater than 200 MΩ then pipette tips were beveled in a jet stream containing 0.05 μm gamma alumina particles until tip resistance fell below 200 MΩ. HRP was ejected by passing a positively DC offset 4 Hz sinusoidal current of 0.5 to 1 nA and Lucifer was ejected by passing a negatively DC offset current of approximately the same magnitude and frequency.

Since the electric organ of apteronotids is composed of modified spinal motor neurons it is not abolished by curarization, hence animals received the normal continuous input to the electrosensory system. Additional electrosensory stimuli consisted of single cycles of a sinusoidal signal having a period slightly less than that of the animal's electric organ discharge (EOD). Sinusoids were triggered by each successive EOD cycle recorded between the animal's head and tail. Changes in EOD amplitude were produced by adding or subtracting trains of this sinusoid to or from the fish's normal discharge. Stimulus intensity was measured via a bipolar pair of silver wire electrodes, 1 cm spacing, insulated except for the tips. The amplitude of the stimulus was set to 3.75 mV/cm rms without the fish in the recording tank and various stimulus amplitudes were produced by passing this signal through a Hewlett Packard 350D step attenuator. The stimulus was isolated from ground with an isolation transformer and delivered to the fish either with electrodes mounted on the tank walls on either side of the fish (transverse geometry) or between an electrode inserted into the mouth and a second electrode near the tip of the tail (mouth-tail geometry).

In experiments in which brain regions were directly stimulated, bipolar electrodes made from 40 μm insulated stainless steel wire were used to deliver constant current pulses of 50 μs duration and amplitudes of 10 to 50 μA.

Intracellularly recorded data, the animal's electric organ discharge, and stimulus synchronization pulses were stored on magnetic tape (Hewlett Packard model 3960, 3.75 ips, FM mode). Resting firing frequencies were determined from interval histograms. The relationship between times of action potential occurrence and the EOD was summarized as histograms of the phase firing within period of the EOD waveform. The intensity of the phase relationship was determined by computing the mean vector or vector strength (Batschelet 1981). This statistic ranges from 0 for random timing of events relative to a reference signal to 1.0 for perfect synchronization.

Responses to electrosensory stimuli were summarized as raster displays, post stimulus time histograms (PSTH), or plots of spike frequency, determined over successive 100 ms epochs, versus elapsed time. The latter plots were smoothed with a simple digital filter (Bastian 1986b). Response latency was measured as the delay between the onset of a stimulus and the beginning of high-frequency firing. Adaptation time constants were determined from the plots of spike frequency versus time. These were calculated as the negative reciprocal of the slope of the best-fit line relating the natural log of

spike frequency to elapsed time over the 500 ms following the onset of a stimulus. Averages are given along with ±1 S.E.M. unless indicated otherwise.

Results

Anatomy of ELL commissural connections

Thirty extracellular injections of HRP were successfully placed into various layers of the ELL, and these typically resulted in both antero- and retrograde labeling of the axonal arborizations and somata of ELL commissural neurons. The ascending output neurons of the ELL, basilar and nonbasilar pyramidal cells, were also labeled as has been shown previously (Maler et al. 1982). In the example shown in Fig. 1A the injection, indicated by the asterisk, was confined to the pyramidal through granule cell layers of the centrolateral ELL segment. Apical dendrites of pyramidal and polymorphic cells are filled within the dorsal and ventral molecular layers (mol) and sweep dorsomedially. Although this injection was confined to the centrolateral segment of the ELL, a dense fiber plexus is seen within the granule cell layers of the lateral and centromedial segments bordering the injected segment. Within the contralateral ELL centrolateral segment a network of labeled axons fills the ventral granule cell layer, and fascicles of labeled processes ascend to about the top of the granule cell layer where most abruptly stop (Fig. 1A, arrow). Fewer fibers ascend into the polymorphic cell layer, and those that do remain within its ventral portion. Labeled axons are also seen in the contralateral lateral and centromedial segments and these also give rise to ascending branches identical to those of the centrolateral segment.

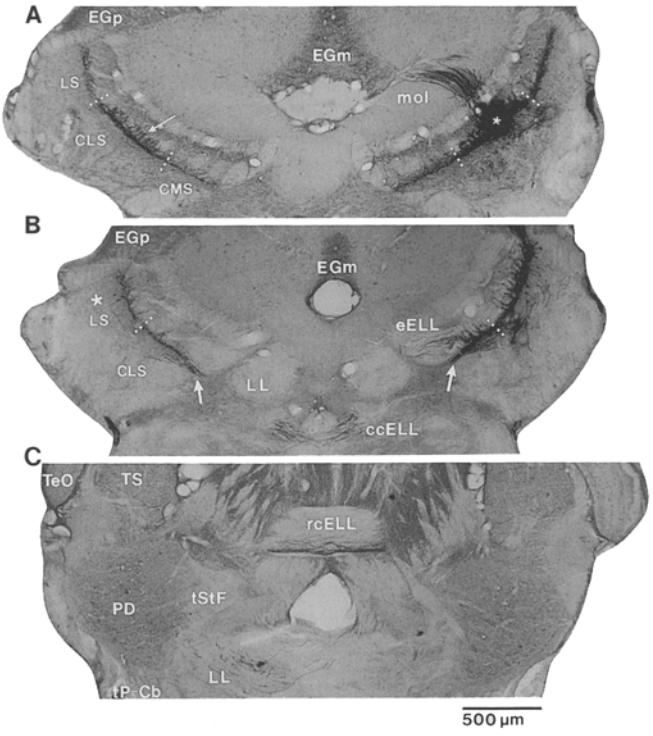

Fig. 1. A Transverse section through the ELL showing the site of an HRP injection (*asterisk*) and the contralaterally filled axonal arborizations. **B** Transverse section approximately 360 µm rostral to **A** showing the decussation of the caudal commissure of the ELL, the sites at which caudal commissure fibers exit the ELL (*arrows*), and 2 retrogradely labeled ovoid cells (*asterisk*). **C** Transverse section approximately 720 µm rostral to that of **B** showing the decussation of the rostral commissure of the ELL. The sections of **A–C** correspond to atlas levels −5, −3, and 4, respectively, of Maler et al. (1991). *ccELL*, caudal commissure of the ELL; *CLS*, centrolateral segment; *CMS*, centromedial segment; *eELL*, efferent of the ELL; *EGm*, medial eminentia granularis; *EGp*, posterior eminentia granularis; *LL*, lateral lemniscus; *LS*, lateral segment; *mol*, molecular layers; *PD*, nucleus praeeminentialis; *rcELL*, rostral commissure of the ELL; *TeO*, optic tectum; *TS*, torus semicircularis; *tStF*, tractus strati fibrosi

The high density of label in the centrolateral segment opposite the injected ELL compared to that in neighboring contralateral segments suggests that the commissural connections may predominantly, or perhaps exclusively, be between corresponding segments. Dense injections such as shown in Fig. 1A cause localized tissue damage and the presence of label in the neighboring segments, both ipsilaterally and contralaterally, may be due to HRP uptake by damaged axons coursing through the injection site. That individual commissural axons ramify exclusively within a single ELL segment is clearly shown by the results of single cell recording and labeling experiments described later.

The caudal ELL commissure

The axons labeled in Fig. 1A are subdivided into two populations which take different routes to the contralateral ELL. A group of thick fibers, roughly 3 to 5 µm in diameter, coalesces into a tight bundle and exits the rostral ELL (arrows in Fig. 1B) just ventral to the large bundle of pyramidal cell axons, the efferents of the ELL (eELL), that enter the lateral lemniscus. The thick fibers continue from the sites of the arrows, running ventrally and medially, ultimately crossing the midline within the caudal commissure of the ELL (ccELL) shown in Fig. 1B. The ccELL fibers loop caudally about 300 µm from the level of Fig. 1B, so the connections between the axons shown at the arrows and the ccELL are distributed over 5 more caudal sections. The approach of these axons to the midline is summarized as the black band in the diagram of Fig. 2A. This diagram corresponds to rostrocaudal level −3 from the atlas of the brain of *Apteronotus leptorhynchus* (Maler et al. 1991). The caudal commissure of the ELL is distinct from the previously described decussation of the medial segment of the ELL (Maler et al. 1982); the latter crosses the midline about 200 µm caudal to the level of the section of Fig. 1B. When HRP injections are contained within the ELL medial segment no fibers are labeled in the ccELL but the decussation of the medial segment is heavily labeled.

The rostral ELL commissure

The second population of ELL commissural fibers consists of smaller axons, 1 to 2 µm in diameter, which run in

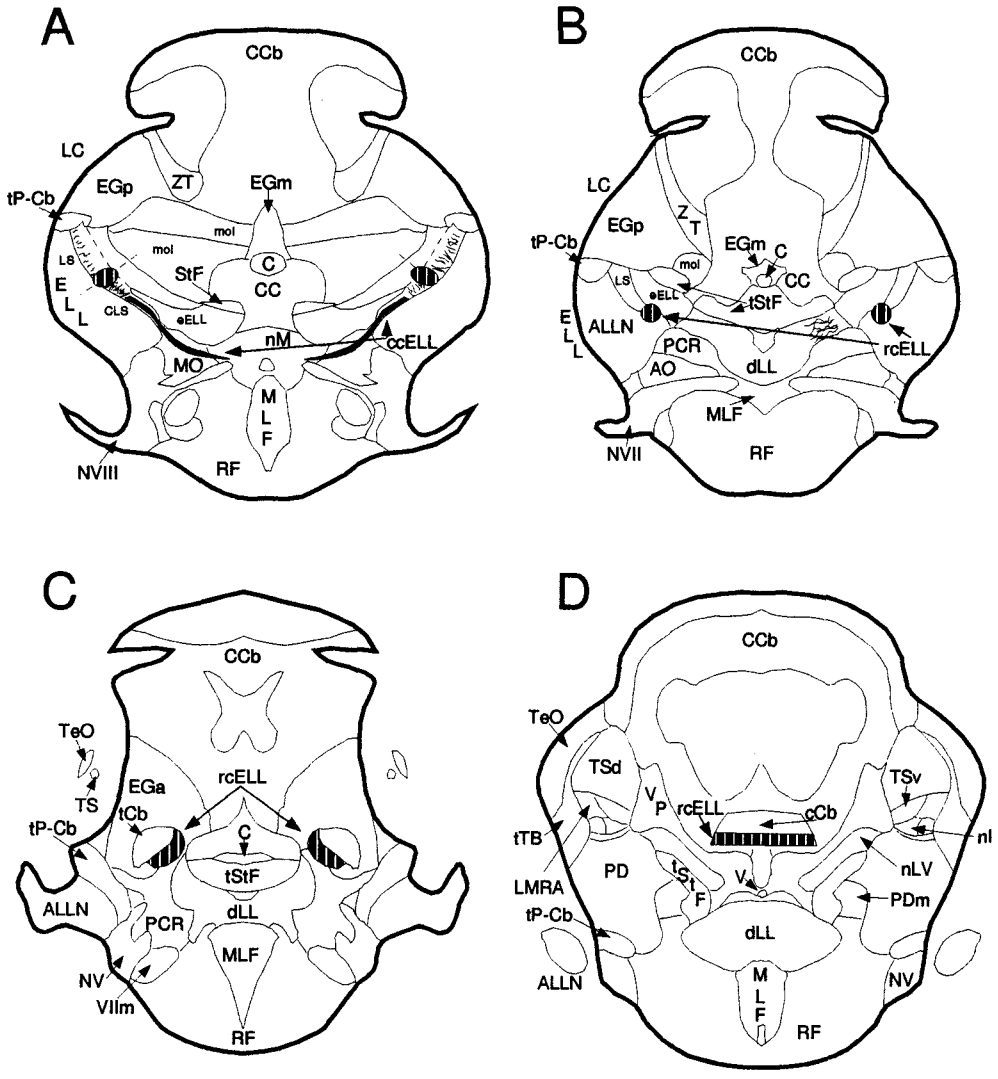

Fig. 2A–D. Diagrams of a caudal to rostral sequence of transverse sections showing the courses taken by fibers of the caudal commissure (*black*) and the rostral commissure (*vertical bars*). Sections **A–D** correspond to atlas levels −3, −1, 1, and 4 of Maler et al. (1991). *ALLN*, anterior lateral line nerve; *AO*, anterior octavolateral nucleus; *C*, cerebello-medullary cistern; *CC*, crista cerebellaris; *CCb*, corpus cerebelli; *cCb*, cerebellar commissure; *ccELL*, caudal commissure of the ELL; *CLS*, centrolateral segment; *dLL*, decussation of the lateral lemniscus; *eELL*, efferents of the ELL; *EGa*, anterior eminentia granularis; *EGm*, medial eminentia granularis; *EGp*, posterior eminentia granularis; *ELL*, electrosensory lateral line lobe; *LC*, caudal lobe of the cerebellum; *LMRA*, lateral mesencephalic reticular area; *LS*, lateral segment; *MLF*, medial longitudinal fasciculus; *MO*, medial octavolateral nucleus; *mol*, molecular layers; *nI*, nucleus isthmi; *nLV*, nucleus lateralis valvula; *nM*, nucleus medialis; *NV*, trigeminal nerve; *NVII*, facial nerve; *NVIII*, vestibular cochlear nerve; *PCR*, paracommissural region; *PD*, dorsal nucleus praeeminentialis; *PDm*, medial nucleus praeeminentialis; *rcELL*, rostral commissure of the ELL; *Stf*, stratum fibrosum; *tCB*, cerebellar tract; *TeO*, optic tectum; *tp-Cb*, tractus praeeminentialis cerebellaris; *TSd*, dorsal subdivision of torus semicircularis; *tStF*, tractus strati fibrosi; *TSv*, ventral subdivision of torus semicircularis; *tTB*, tectobulbar tract; *V*, ventricle; *VP*, valvular peduncle; *ZT*, transitional zone of lobus caudalis

a small bundle at the junction of the centrolateral and lateral ELL segments. This tract is shown as the elliptical area filled with vertical bars in Fig. 2A and a higher magnification view of this structure is shown in Fig. 3A (surrounded with double arrows). This fiber bundle ultimately forms the rostral commissure of the ELL (rcELL). It exits at the rostromedial ELL boundary (Fig. 2B), then runs rostrally apposed to the medial edge of the cerebellar tract (tCb, Fig. 2C). The rcELL turns medially at about the level of cerebellar commissure (atlas level 4; Maler et al. 1991) and crosses the midline as a ventral subdivision of this structure (Figs. 1C, 2D). We have never observed that axons forming the rostral commissure of the ELL branch, neither have others using more sensitive tracers (L. Maler, personal comm.), hence this long pathway is exclusively a projection to the contralateral ELL.

Commissural cell types

The HRP injections also retrogradely labeled at least 3 morphologically distinct cell types within the contralateral ELL. Ovoid cells, first described by Maler (1979), were densely labeled and typically occurred within the

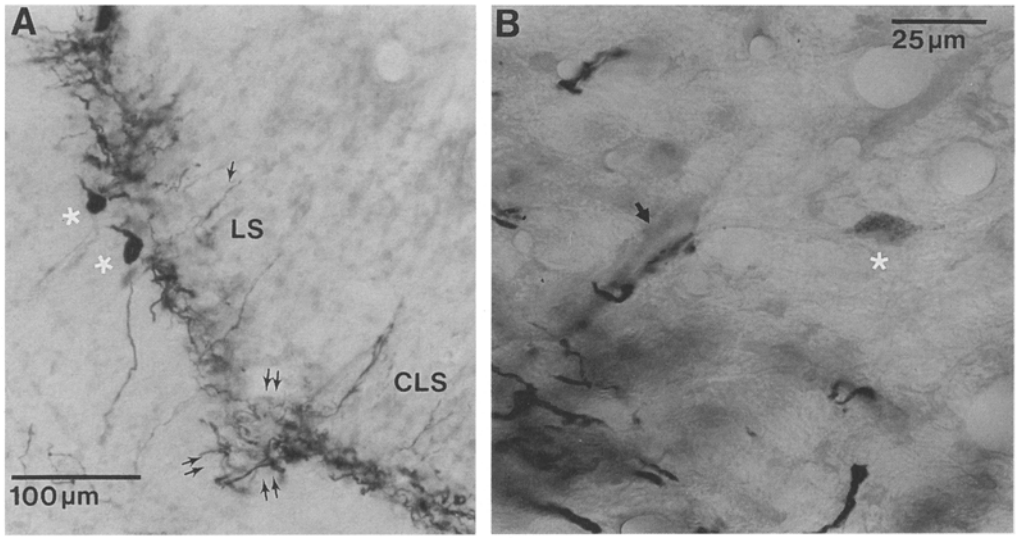

Fig. 3. A Retrogradely labeled ovoid neurons (*asterisks*) resulting from HRP injection to the contralateral ELL centrolateral segment. Sets of *double arrows* show the position of ELL efferent fibers that give rise to the rostral ELL commissure. **B** Retrogradely labeled polymorphic cell (*asterisk*) resulting from an HRP injection in the contralateral ELL. Probable synaptic contacts between filled commissural fibers and various ELL neurons are also visible, including contacts with a deep basilar pyramidal cell (*arrow*). *LS*, lateral segment; *CLS*, centrolateral segment

deep fiber layer of the lateral and centrolateral segments just below the commissural axons (Figs. 1B, 3A asterisks). Ovoid cells were also seen in the centromedial segment but in this segment they were confined to the ventral region of the granule cell layer. In well filled cases ovoid cell dendrites could be seen traveling over long distances within the deep fiber layer. Cells similar to the multipolar cells of Szabo and Fessard (1974) and Maler (1979) were rarely seen at about the same level within the ELL. The polymorphic cell of Maler (1979) was the third ELL cell type that was retrogradely labeled. Polymorphic cells are found scattered at most levels within the ELL cell layers and an example is shown in Fig. 3B (asterisk). Polymorphic cells were retrogradely labeled following HRP injections to any of the 4 ELL segments and, as observed earlier (Maler et al. 1982), these cells were never as strongly labeled as were the ovoid cells.

Polymorphic cells have apical dendrites which extend into the dorsal molecular layer (DML) but ovoid and multipolar cells lack apical dendrites. Horseradish peroxidase injections limited to the DML labeled polymorphics but not the latter categories, and such injections labeled axons within the rostral ELL commissure and contralateral polymorphic cells, but never labeled the ovoid cells, multipolar cells, or fibers of the caudal commissure. Hence, only polymorphic cells project via the rostral commissure and the long projection pathway plus the relatively thin axonal diameter may account for our inability to strongly label these cells. The ovoid and multipolar cells project via the caudal commissure, and in the case of the ovoid cells, this projection is verified by single cell recording and labeling studies described later. These same projection patterns have been observed by Maler and Mugnaini (personal comm.) in conjunction with a study of GABAergic circuitry of these fish.

Of the 30 successful extracellular HRP injections, 3 were predominantly within the lateral segment, 9 were within the centrolateral segment, 15 were within the centromedial segment and 3 were within the medial segment. No differences were seen in the patterns of labeling resulting from injections in the lateral 3 tuberous or high-frequency receptor afferent recipient segments. When the injection was restricted to the molecular layers (7 of the 27 tuberous map injections) the caudal commissure was never labeled but the rostral pathway always was. Thirteen of the remaining 20 tuberous map injections impinged on the ELL cell layers and in these cases both commissures were labeled. In the remaining cases the injections were quite ventral within the deep fiber layer and although receptor afferent axons were strongly labeled, neither commissure was. The 3 medial segment (ampullary receptor recipient map) injections labeled both the rostral commissure of the ELL and the decussation of the medial segment, but no fibers were seen in the caudal commissure. Cells similar to the polymorphic cells seen in the lateral 3 segments are weakly retrogradely labeled following medial segment injections and these may give rise to the rostral commissure fibers. Ovoid and multipolar cells are seen in the deep layers of the medial segment ipsilateral to the injection site, but none were retrogradely labelled. The lack of labelled fibers in the caudal commissure may indicate that the ovoid and multipolar cells project via the decussation of the medial segment along with axons of the medial segment pyramidal cells. Additional studies of the projection patterns of medial segment neurons are clearly needed.

Most extracellular HRP injections, and the intracellular injections described below, intensely labeled axon terminals and terminal boutons enabling us to speculate as to the synaptic targets of the commissural fibers. When caudal commissure fibers were filled compact fascicles of fibers ascended vertically from the parent axons located at the boundary of the deep fiber layer and the ventral granule cell layer (Figs. 1A, 3A; single arrows). Single ovoid cell fills also resulted in similar vertical fibers being labeled (Figs. 7A, 8A). The branches of ovoid cell axons appeared to make extensive synaptic contact with deep basilar pyramidal cells and the basilar dendrites of basilar pyramidal cells but filled fibers never approached the vicinity of nonbasilar pyramidal cells. The dorsoventral position of basilar pyramidal cells is variable (Bastian and Courtright 1991) and those found deeper within the

polymorphic cell layer may also receive dense somatic contacts from ovoid cells (Fig. 3B, arrow). Terminals were also seen apposed to small cells within the granule cell layer suggesting that the ovoid cell axons may make synaptic contact with one or both types of granule cells which are inhibitory interneurons.

HRP injections limited to the ELL molecular layers only filled fibers within the rostral commissure and in these cases vertically oriented fascicles of fibers were not filled. Instead a more diffuse collection of thinner fibers restricted to the granule cell layer was filled and these probably contact granule cells. Neither basilar, deep basilar, nor nonbasilar pyramidal cells seemed to receive contacts from rostral commissure fibers.

Physiological characteristics of ovoid neurons

Intracellular recordings made within the granule cell layer, just above the deep fiber layer, revealed units with extremely consistent properties. The action potentials rose from a flat baseline, there was usually no indication of synaptic events, and firing frequency was rarely altered by intracellular current injection indicating that most recordings were from axons rather than from cell bodies. The cells had very high rates of resting activity; firing frequency in response to the normal electric organ discharge averaged 73.5 ± 0.16 spikes/s for a sample of 25 cells, and interval histograms of this activity were bell shaped (Figs. 4A, 7B, 8B, 9B) instead of being skewed toward longer intervals as is typical of ELL pyramidal cells (Bastian 1981; Bastian and Courtright 1991). Instead of being continuous, the interval histograms were usually subdivided into a collection of narrower peaks, and the interval between these was approximately equal to the EOD interval. This property suggests a strong phase coupling to the electric organ discharge waveform.

Phase histograms, such as that of Fig. 4B, summarize a cell's times of firing relative to the EOD cycle and the mean vector, or vector strength (Batschelet 1981) was used to quantify the intensity of phase coupling. This measure ranges from zero for firing at random relative to the reference signal to one for perfect phase coupling. Averages of vector strength for receptor afferents, fibers such as that of Fig. 4 recorded within the ELL granule cell layer, and the two classes of ascending ELL output cells, basilar and nonbasilar pyramidal cells, are summarized in Fig. 5A. As described earlier (Hagiwara et al. 1965), receptor afferents fire with a high degree of phase coupling to the EOD waveform; vector strength averaged 0.88 ± 0.02. The basilar pyramidal cells' activity is much less tightly coupled to the EOD (vector strength averaged 0.33 ± 0.05) and the nonbasilar pyramidal cells' phase histograms are virtually flat (vector strength averaged 0.14 ± 0.03).

The fibers recorded in these experiments can be subdivided into two groups as described below. Both types' firing was highly synchronized to the EOD waveform (vector strengths averaged 0.73 ± 0.04 and 0.74 ± 0.05 for ipsilaterally and contralaterally excited cell types, respectively). This high degree of synchrony shows that these units preserve nearly as much information about the timing of the electric organ discharge as do the receptor afferents.

All ELL cells showing this high degree of phase coupling to the EOD waveform responded with similar dynamics to stepwise changes in EOD amplitude, but could be subdivided into two populations depending on the stimulus polarity that evoked excitatory responses. Electrosensory stimuli affect various regions of the body differently depending on the geometry with which they are presented. When the stimulus is presented transversely, perpendicular to the long axis of the fish, the imposed field generates voltage changes of opposite polarity

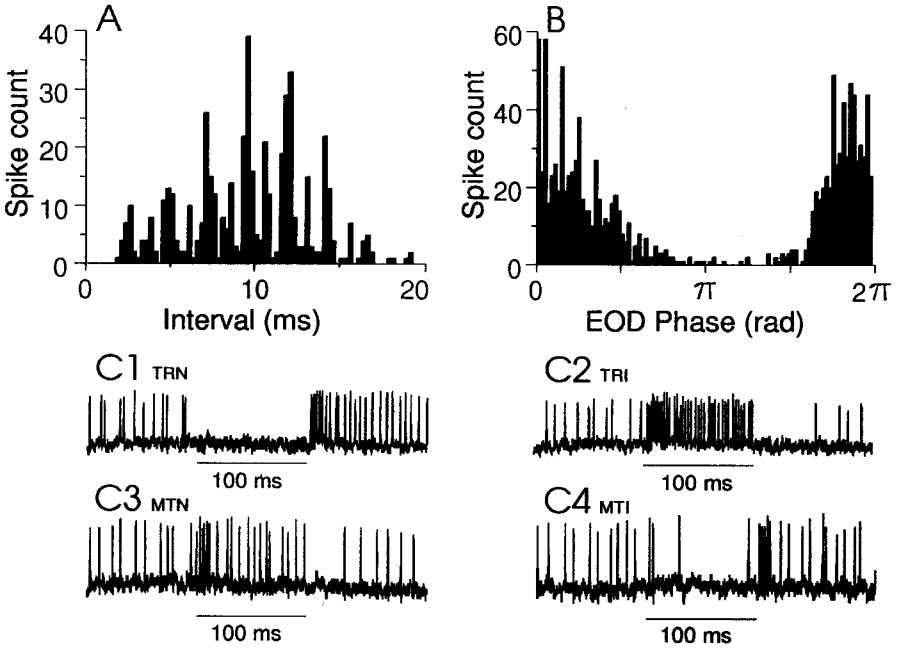

Fig. 4. **A** Interval histogram of an ELL ovoid cell axon recorded within the ELL granule cell layer firing in response to the undisturbed electric organ discharge. The average spike interval corresponds to a frequency of 104.2 spikes/s. **B** Histogram summarizing the phase of this unit's firing relative to the EOD cycle. Zero radians corresponds to the positive going zero-crossing of the EOD waveform. Vector strength for this histogram was 0.67, and the EOD interval averaged 1.2 ms. **C1–4** show responses of this neuron to 100 ms, 0.375 mV/cm rms changes in EOD amplitude presented with transverse normal (*TRN*), transverse inverted (*TRI*), mouth-tail normal (*MTN*), and mouth-tail inverted (*MTI*) geometries, respectively

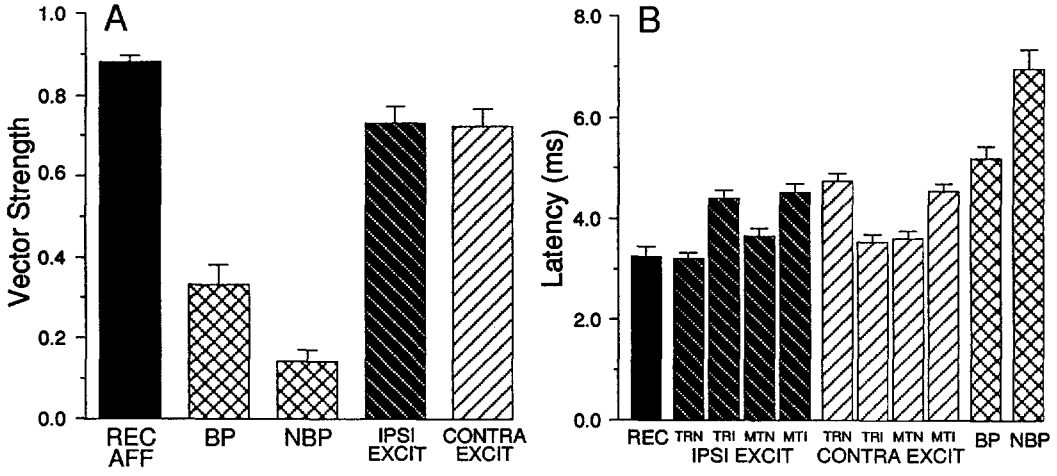

Fig. 5. **A** Summary of average vector strengths, plus 1 S.E.M., determined from histograms like that of Fig. 4B for the resting firing pattern of receptor afferents (*REC AFF*, $n=6$), basilar pyramidal cells (*BP*, $n=16$), nonbasilar pyramidal cells (*NBP*, $n=7$), ipsilaterally excited ELL commissural fibers (*IPSI EXCIT*, $n=12$), contralaterally excited fibers (*CONTRA EXCIT*, $n=13$). **B** Summary of average response latency, plus 1 S.E.M, for receptor afferents and the indicated ELL cell types to 0.375 mV/cm changes in EOD amplitude. Receptor afferents (*REC*, $n=25$), ipsilaterally excited fibers (*IPSI EXCIT*, $n=48$), contralaterally excited fibers (*CONTRA EXCIT*, $n=45$), basilar pyramidal cells (*BP*, $n=87$), nonbasilar pyramidal cells (*NBP*, $n=50$). Receptor afferents and basilar pyramidal cells were stimulated with transverse normal stimuli, nonbasilar pyramidal cells with transverse inverted stimuli, and the ELL fibers were stimulated with transverse normal (*TRN*), transverse inverted (*TRI*), mouth-tail normal (*MTN*), and with mouth-tail inverted (*MTI*) geometries

across the skin on opposite sides of the body. Hence, stimuli causing increased receptor afferent activity on a given side simultaneously cause reduced activity on the opposite side. Such stimuli are defined as 'transverse normal' (TRN) for the polarity resulting in increased receptor afferent activity ipsilateral to the ELL recorded from coupled with reduced activity contralaterally. Reversing the polarity of the signal, 'transverse inverted' (TRI), results in increased receptor activity contralateral to the ELL recorded from and decreased activity ipsilaterally. Electrosensory stimuli can also be applied between an electrode inserted into the animal's mouth and one placed at the tip of the tail. This geometry results in symmetrical increases or decreases in receptor afferent activity over the majority of the body surface. Hence, 'mouth-tail normal' stimuli (MTN) result in increased receptor afferent activity both ipsilateral and contralateral to the ELL and 'mouth-tail inverted' (MTI) refers to stimuli that decrease afferent activity symmetrically.

One category of fiber responded to ipsilateral increases coupled with contralateral decreases in receptor afferent activity (TRN stimuli) with reduced firing (Figs. 4C1, 8C1). These cells responded to the termination of this stimulus with a brief high frequency burst which declined approximately exponentially to the cell's resting firing rate. The opposite stimulus, transverse inverted, evoked a short-latency burst which only partially adapts (Figs. 4C2, 8C2). These response patterns could arise if the cell studied received inhibitory inputs, driven by receptor afferents, from the ipsilateral side of the body or if the recorded cell received excitatory input, directly from, or driven by, receptor afferents from the contralateral side. These alternatives can be distinguished by using the mouth-tail geometry which symmetrically increases or decreases receptor afferent activity. Since the cell of Fig. 4 was excited by symmetrical increases in EOD amplitude (MTN stimuli) and responded with reduced firing to MTI stimuli (Fig. 4C3,C4), it is most likely driven by receptor afferents innervating the contralateral ELL. Cells responding in this manner will be referred to as contralaterally excited or CE cells.

Approximately 50% of the units recorded having spontaneous firing characteristics similar to those described above responded oppositely to the transversely applied stimuli. These were excited by ipsilateral increases in EOD amplitude coupled with contralateral decreases (TRN stimuli) and showed reduced firing due to TRI stimuli (Fig. 7C1,C2). Since these units were also excited by symmetrical (MTN) and silenced by MTI stimuli (Fig. 7C3,C4) it is likely that they receive excitatory input from an ipsilateral population of receptor afferents. These are referred to as ipsilaterally excited (IE) cells.

Both IE and CE cells responded to excitatory stimuli with very short latencies. Their average response latencies to the excitatory phase of stimuli presented with different geometries, along with mean latencies of receptor afferents, and basilar and nonbasilar pyramidal cells are summarized in Fig. 5B. Basilar and nonbasilar pyramidal cell average latencies were significantly longer than that of receptor afferents ($P<0.002$ in both cases, t-test corrected for multiple comparisons). However, neither the mean response latency of ipsilaterally excited cells to the transverse normal stimuli, nor that of the contralaterally excited cells to the transverse inverted stimuli, were significantly longer than average receptor afferent latency. Receptor afferent latency averaged 3.25 ± 0.2 ms, that of IE cells to TRN stimuli averaged 3.13 ± 0.13 ms, and that of CE cells to TRI stimuli averaged 3.55 ± 0.16 ms ($P>0.86$ and $P>0.24$, for t-tests comparing IE and CE cells, respectively, with receptor afferents). The short la-

tency of the IE and CE cells' responses and the strong phase coupling between the EOD waveform and the times of action potential occurrence are probably due to the gap junction input to these cells from receptor afferents (Maler et al. 1981; Yamamoto et al. 1989). Response latencies to the symmetrical increases in EOD amplitude (MTN stimuli) were also very short, but the response latencies to the excitatory phase (cessation) of the non-preferred stimuli were significantly longer than those to the onset of preferred stimuli (Fig. 5B).

Responses of a contralaterally excited cell to long-duration (5 s) increases in EOD amplitude presented via the transverse inverted and the mouth-tail normal geometries are shown in Fig. 6A,B as plots of spike frequency versus elapsed time. Responses to the same four stimulus intensities are shown in each plot and in all but the weakest cases the responses show a phasic and tonic component. The initial response decays rapidly to a plateau level of activity that is greater than the cell's resting firing frequency. Both the rate and degree of adaptation were usually greater for stimuli applied with the mouth-tail geometry. Adaptation time constants were computed from the first 500 ms of the responses to the two largest stimulus amplitudes used (−10 and −20 dB; 1.19 and 0.375 mV/cm rms). These were not significantly different contingent upon cell type, IE or CE, nor were they different for stimulus intensities presented with a given geometry. These averaged 0.51 ± 0.042 ms ($n=13$) and 0.51 ± 0.067 ms ($n=16$) for −10 and −20 dB stimuli, respectively, applied with the preferred transverse geometry. Time constants were significantly less for both −10 and −20 dB stimuli presented with mouth-tail geometry, averaging 0.34 ± 0.048 ms ($n=6$) and 0.28 ± 0.069 ms ($n=8$), respectively ($P \leq 0.05$, t-tests).

Peak increases in spike frequency above resting activity and the adapted response (average firing frequency during the last second of stimulation) are plotted as function of stimulus amplitude in Fig. 6C and D for transverse and mouth-tail stimuli. Both the peak and late responses, circles and triangles, respectively, are greater for the transversely applied stimuli.

Morphological characteristics of ovoid cells

HRP or Lucifer yellow filled micropipettes were used in most experiments so that the units recorded intracellularly could be morphologically identified. Figure 7A shows a partial reconstruction of an HRP filled axon that had spontaneous firing characteristics and responses to electrosensory stimuli typical of the ipsilaterally excited cells. Reconstruction revealed an enormous axon plexus which coursed throughout most of the rostro-caudal extent of the ELL. The parent axon was located near the ventral margin of the granule cell layer and gave off ascending branches which were identical to those seen following the extracellular HRP injections. This fiber plexus was located within the centrolateral ELL segment and no process-

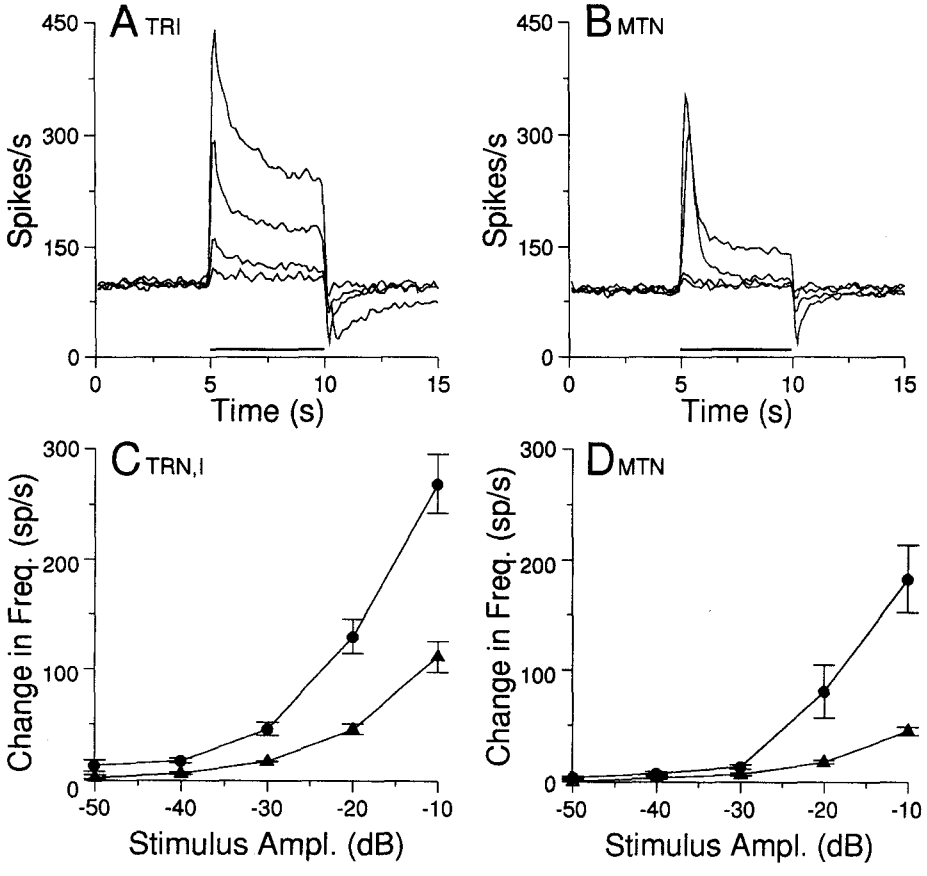

Fig. 6. A,B Responses of a contralaterally excited cell to 5 s changes in EOD amplitude presented with transverse inverted (*TRI*) and mouth-tail normal (*MTN*) geometries. Stimulus intensities of −10 through −40 dB relative to 3.75 mV/cm rms were used and result in the largest through smallest responses, respectively. **C,D** Average increments in firing frequency over resting activity, ± 1 S.E.M., measured at the peak and over the last second of the response (*circles* and *triangles*, respectively) for transverse and mouth-tail stimulus geometries. Data from 7 ipsilaterally and 7 contralaterally excited fibers are included although responses to each intensity were not available for every cell

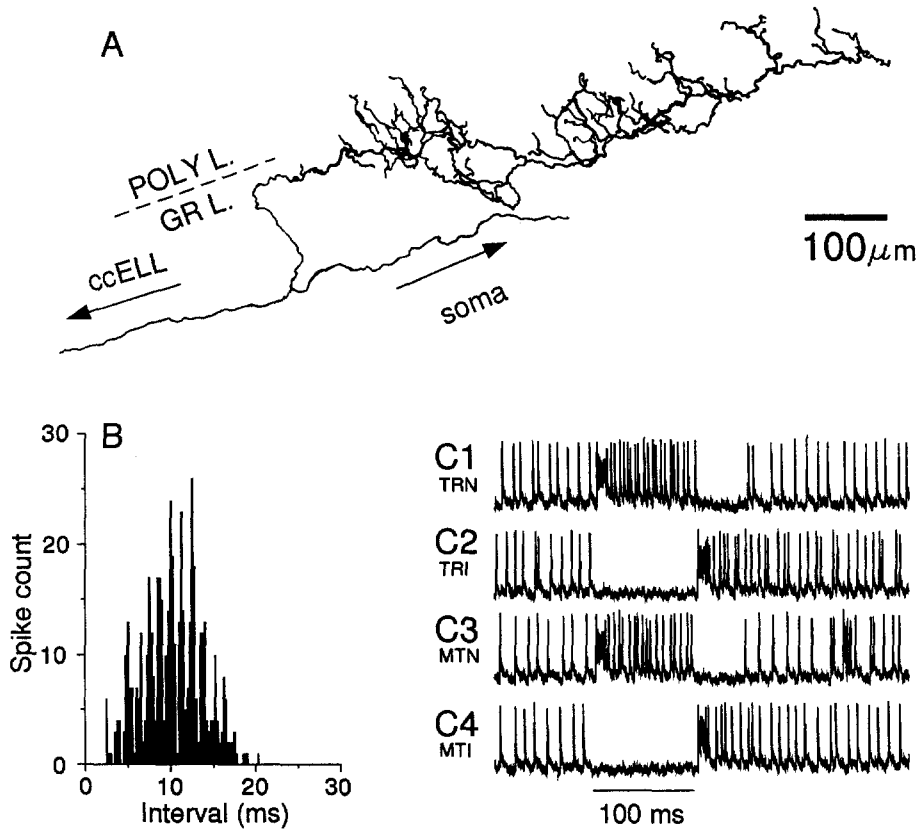

Fig. 7. **A** Reconstruction of an HRP filled fiber that was excited by ipsilateral increases in receptor afferent activity. The arborization was entirely within the centrolateral segment of the ELL and it extended over nearly the entire rostrocaudal extent of the ELL, a distance of approximately 1020 μm. **B** Interval histogram of this fiber's resting activity, average interval corresponds to a frequency of 96.3 spikes/s. **C1–4** Responses of this cell to 0.375 mV/cm rms changes in EOD amplitude presented with transverse normal (*TRN*), transverse inverted (*TRI*), mouth-tail normal (*MTN*), and mouth-tail inverted (*MTI*) geometries

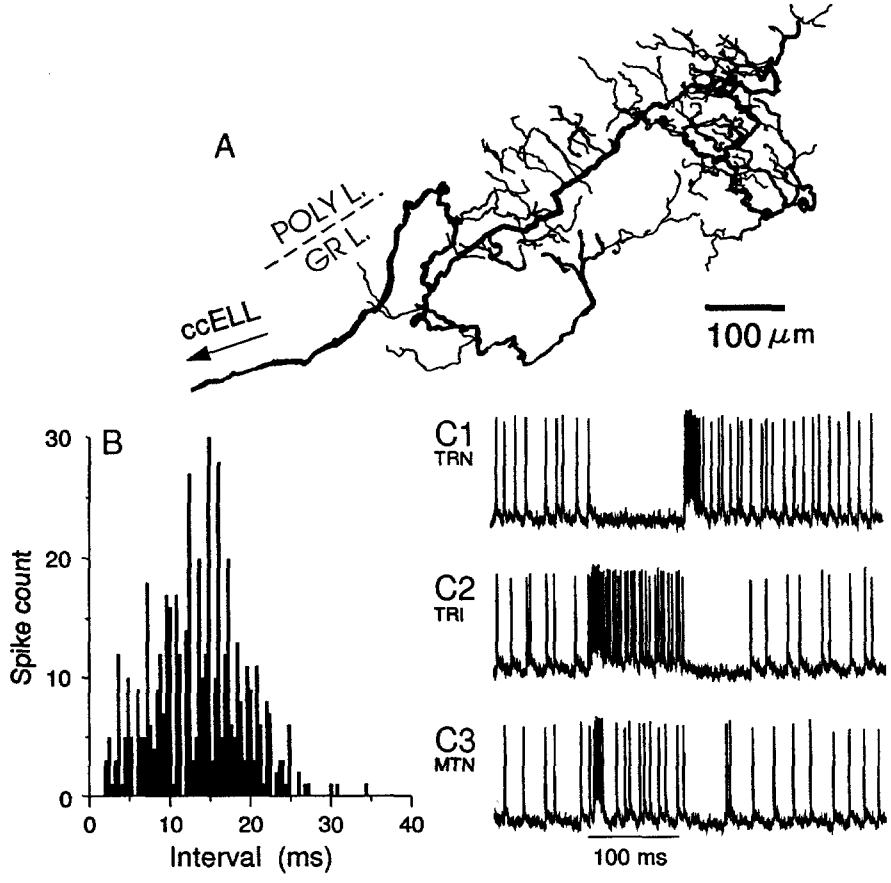

Fig. 8. **A** Reconstruction of an HRP filled fiber that was excited by increased receptor afferent activity contralateral to the ELL recorded from. Rostrocaudal extent of this reconstruction is 1380 μm, it was also restricted to the centrolateral ELL segment. **B** Interval histogram of this cell's resting activity, average frequency = 74.4 spikes/s. **C1–3** Responses of this cell to changes in EOD amplitude of 0.375 mV/cm rms presented with transverse normal (*TRN*), transverse inverted (*TRI*) and mouth-tail normal (*MTN*) geometries

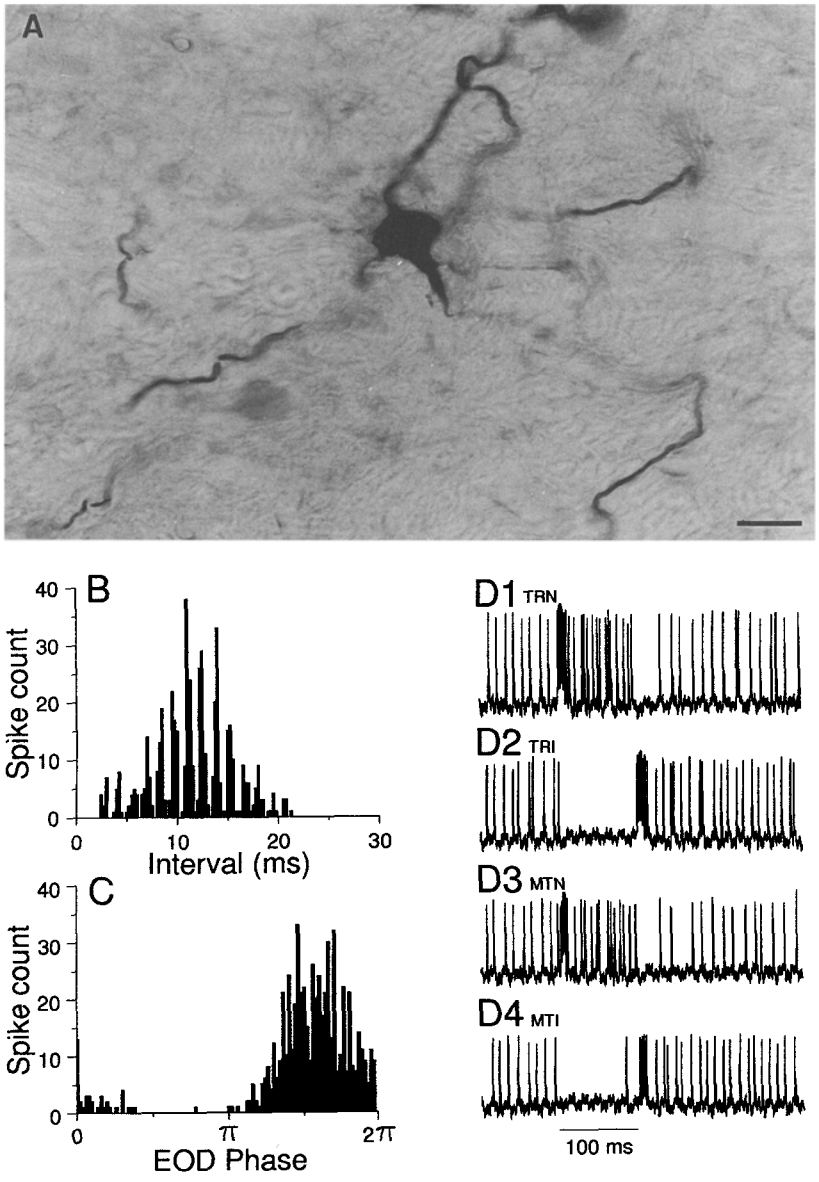

Fig. 9. **A** HRP filled ovoid cell soma recorded within the lateral segment of the ELL, calibration bar indicates 20 μm. Filled fibers are portions of this cell's dendritic field. **B,C** Interval and phase histograms of the filled cell's resting activity. Resting frequency averaged 85.4 spikes/s and the vector strength of this phase histogram is 0.77. **D1–4** Responses of this cell to 0.375 mV/cm rms changes in EOD amplitude presented with transverse normal (*TRN*), transverse inverted (*TRI*), mouth-tail normal (*MTN*), and mouth-tail inverted (*MTI*) geometries

es giving off vertical branches crossed segmental boundaries. The parent axon exited the ELL at its rostromedial boundary as part of the bundle indicated by the arrow in Fig. 1B and it could be followed to within the caudal commissure of the ELL. This axon branched just rostral to the point at which it left the ELL and one branch turned to run caudally toward the lateral segment of the ELL. Although no cell body was labeled by this HRP injection, other fills described later suggest that this recurrent branch joins the axon to its soma.

An interval histogram of this cell's resting activity is shown in Fig. 7B; it shows the multiple peaks characteristic of highly synchronous firing with the EOD waveform. The responses of this cell to the 4 stimulus geometries used are shown in Fig. 7C1–C4. The characteristic bursts during which the cell fires one-to-one with the EOD occur in response to EOD increases, and since transverse normal and mouth-tail normal stimuli are excitatory, this cell must be excited by ipsilateral increases in afferent activity. This neuron's responses to long-term changes in EOD amplitude had time courses similar to those shown in Fig. 6A,B.

Figure 8 summarizes data recorded from another ELL unit that showed the response pattern typical of the contralaterally excited type. Reconstruction (Fig. 8A) showed that this recording was also made from a very large axonal plexus which extended through nearly the entire rostro-caudal length of the ELL. This plexus was also restricted to the centrolateral segment and its general features are similar to those of Fig. 7A except that no recurrent branch was found and the parent axon was of larger diameter than that of Fig. 7A. The interval histogram of the cells's spontaneous activity is also bell-shaped and fragmented into multiple peaks (Fig. 8B). This cell responded with decreased firing frequency to ipsilateral increases in EOD amplitude applied transversely (Fig. 8C1) and was excited by the opposite polarity (Fig. 8C2) which causes increased activation of con-

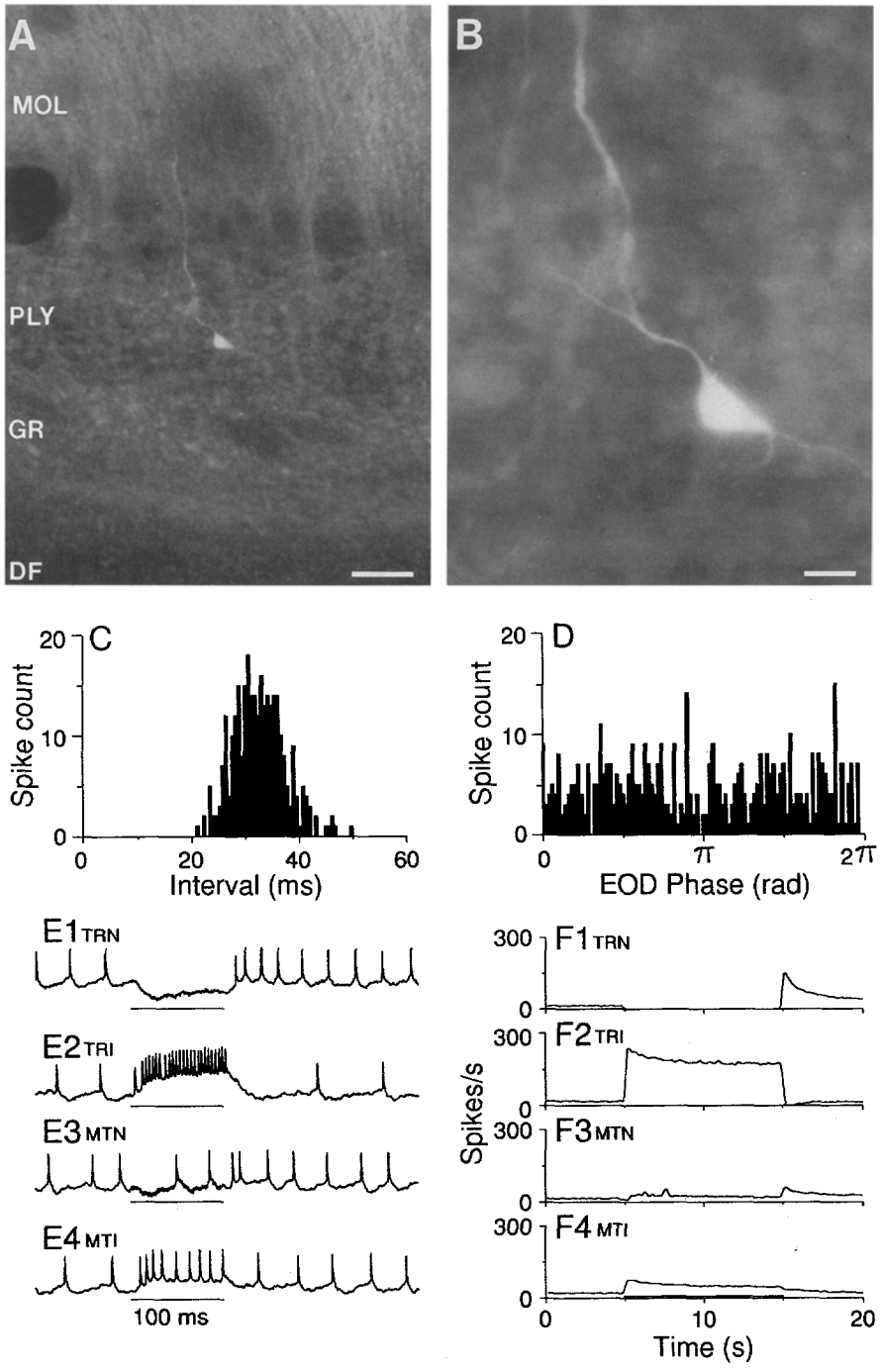

Fig. 10. A,B Low and higher magnification views of a Lucifer yellow filled polymorphic cell. Calibration bars in **A** and **B** indicate 50 and 10 μm, respectively. **C** Interval histogram of resting activity, mean spike frequency = 30.4 spikes/s. **D** Histogram of resting activity relative to the EOD cycle, vector strength = 0.02. **E,F** Responses of the cell shown in **A,B** to brief and long-term changes in EOD amplitude, respectively, presented with transverse normal (*TRN*), transverse inverted (*TRI*), mouth-tail normal (*MTN*), and mouth-tail inverted (*MTI*) geometries. The duration of the long-term stimulus is indicated by the thickened baseline of **F4**. Stimulus amplitude was 1.2 mV/cm rms

tralateral receptors. Since this cell was also excited by symmetrical increases in EOD amplitude (Fig. 8C3) its soma was probably located in the contralateral ELL.

Seven of 13 successful intracellular fills were completed for cells excited by contralateral increases in receptor afferent activity. In these cases axonal arborizations similar to that shown in Fig. 8A were filled. Of the six fills completed for cells excited by ipsilateral increases in EOD amplitude, 3 revealed axonal arborizations similar to that of Fig. 7A and 3 fills labeled the recorded cells' somata. An example of one of these is shown in Fig. 9A; it is identical to that of the ovoid cells previously described by Maler (1979) and to those retrogradely labeled by extracellular HRP injections (see Fig. 3A, asterisks). The interval histogram of this cell's spontaneous activity showing the fragmented distribution is shown in Fig. 9B, and the phase histogram of action potential occurrence relative to the EOD cycle is shown in Fig. 9C. Responses to electrosensory stimuli presented with the 4 different geometries are shown in Fig. 9D1–D4; the characteristic high frequency burst in response to the initial increase in ipsilateral EOD amplitude is obvious and this cell also responded to long-term stimuli (5 s duration) with responses similar to those described in Fig. 6A,B. This neu-

ron's spontaneous firing rate could be modulated by current injection indicating that the impalement was relatively near the spike initiating zone. No synaptic potentials were seen during this cell's responses to electrosensory stimuli although such potentials were seen with other soma recordings. All cases in which somata were filled showed excitatory responses to stimuli which increased ipsilateral receptor afferent activity.

Physiology and anatomy of polymorphic cells

Only 3 polymorphic cells have been recorded from intracellularly and filled thus far, and sufficient physiological data was obtained for 2 of these. Here we provide a preliminary description of their properties. Figure 10A,B shows a low and higher-magnification view of a Lucifer yellow filled polymorphic cell soma and a portion of its apical dendrite. This soma was roughly mid-level within the polymorphic cell layer. Figure 10C,D shows an interval histogram of the cell's resting activity and a phase histogram relating its times of firing to the EOD waveform. This cell fired regularly at a mean rate of 30.4 spikes/s and the vector strength of the phase histogram was 0.02, hence this cell fired randomly with respect to the EOD waveform. The second cell studied had a mean firing frequency of 57.4 spikes/s and its phase histogram gave a vector strength of 0.09. Figure 10E,F summarizes the responses of the cell shown in Fig. 10A,B to 100 ms and 10 s changes in EOD amplitude of 1.2 mV/cm rms, respectively, presented with different geometries. Transverse normal stimuli tonically reduced the cell's firing rate (Fig. 10E1,F1) and the opposite polarity, TRI stimuli, resulted in large tonic increases in firing (Fig. 10E2,F2). Unlike ovoid cells, which in all cases were excited by mouth-tail normal stimuli, the polymorphics were excited by mouth-tail inverted stimuli which cause reduced EOD amplitude on both sides of the body. Since the soma of this neuron was obviously within the ELL recorded from, and since it was inhibited by increases in ipsilateral receptor afferent activity (TRN and MTN stimuli) and excited by ipsilateral decreases in afferent input (TRI and MTI), this type of cell must receive its predominant input from inhibitory interneurons which are driven by ipsilateral electroreceptor afferents. The long latency of polymorphic responses to excitatory stimuli, 9.6 ms for the cell of Fig. 10 and 7.9 for the second case, is consistent with a disynaptic pathway and is similar to the latencies measured for nonbasilar pyramidal cells (Fig. 5B). The vector strengths of the polymorphic cells' phase histograms are also small as are those of nonbasilar pyramidal cells which receive their main synaptic input from inhibitory interneurons (Maler et al. 1981).

Effects of commissural cell activity on ELL output cells

Experiments were done to determine the effects of increased activity in the commissural pathways on the be-

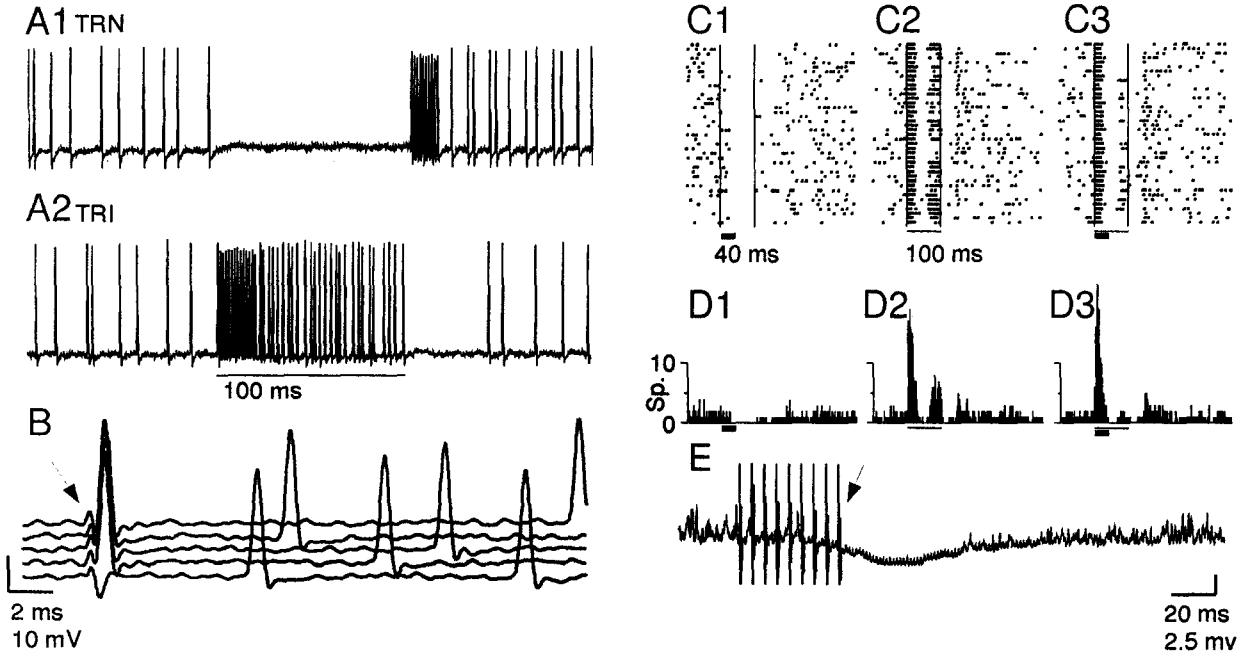

Fig. 11. A1,A2 Responses of a contralaterally excited ovoid cell axon to 0.375 mV/cm rms changes in EOD amplitude presented with transverse normal (*TRN*) and transverse inverted (*TRI*) geometries. **B** Five replicates of this cell's response to electrical stimulation in the rostral contralateral ELL. The *arrow* indicates the stimulus artifact. **C1,D1** Raster display and PSTH of a basilar pyramidal cell's response to a 40 ms train of 20 μA, 50 μs stimuli with a pulse repetition rate of 200 pulses/s delivered at the same site that resulted in the ovoid cell responses shown in **B**. Time of stimulation is shown by the *thick line* below each display. **C2,D2** Responses of this cell to a 100 ms duration increase in EOD amplitude of 0.375 mV/cm rms applied at the time indicated by the horizontal line below each display. **C3,D3** Responses of this cell to the combination of the electrosensory stimulation and the commissural stimulation. **E** Signal average of 50 replicates of intracellular recordings of the BP cell's response to the commissural fiber stimulation. *Arrow* points to the last stimulus artifact in the stimulus train

havior of ELL basilar and non-basilar pyramidal cells. Bipolar stimulating electrodes were positioned in the rostro-lateral ELL near the site at which the ovoid cell axons leave the ELL. An ovoid cell axon was recorded from contralateral to the stimulation site and the position of the bipolar electrodes was adjusted while delivering stimuli. With successful placement of the bipolar electrode, activity could be evoked in the ovoid cell axon recorded from. Both IE and CE ovoid cells were activated by this technique.

Figure 11A,B shows the typical effects of caudal commissure stimulation on an ovoid cell. This neuron was excited by contralateral EOD increases and its responses to transverse normal (TRN) and transverse inverted (TRI) stimuli are shown in Fig. 11A1,A2, respectively. Figure 11B shows 5 responses to single 50 μs, 30 μA stimuli; the timing of which is shown by the arrow. Intensity was near threshold and the stimulus shown in the lowest trace failed to evoke a spike. The next 4 stimuli evoked single spikes with very short latencies.

Following the placement of the bipolar stimulating electrode at a site at which ovoid cells could be stimulated, either intra- or extracellular recordings were made from basilar or nonbasilar pyramidal cells. Fourteen basilar and 8 nonbasilar pyramidal cells were studied. Forty ms trains of stimuli, 200 pulses/s, applied to the site at which the ovoid cell of Fig. 11B was excited, resulted in the changes in basilar pyramidal cell behavior shown in Fig. 11C–E. Commissure stimulation caused a pause in the BP cell's spontaneous activity as shown in the raster display and PSTH of Fig. 11C1,D1. This cell's responses to 100 ms increases in EOD amplitude (TRN stimulation) are shown in Figure 11C2,D2. When the commissure stimulation was paired with the electrosensory stimulus the late phase of the response to the TRN stimulus was attenuated (Fig. 11C3,D3). The initial responses of basilar pyramidal cells to strong electrosensory stimuli, such as shown in Fig. 11, were not affected by commissure stimulation. However, initial responses to weaker stimuli were attenuated. The data of Fig. 11C–D were recorded intracellularly and hyperpolarization of the BP cell was evident as a result of commissure stimulation as shown by Fig. 11E. This record is an average of 50 replicates of the commissure stimulus presented alone. A hyperpolarization of 2–3 mV appears and it is sufficient to prevent the cell from firing for a period of about 70 ms. Averaging accentuates the size of the stimulus artifacts (arrow) and the noisy regions of the trace show the 'averaged' spikes that occurred before and after the hyperpolarization.

The effects of commissure stimulation on nonbasilar pyramidal cell activity was opposite to that seen for basilar pyramidal cells. The inhibitory responses of a NBP cell to increased receptor afferent activity are shown in

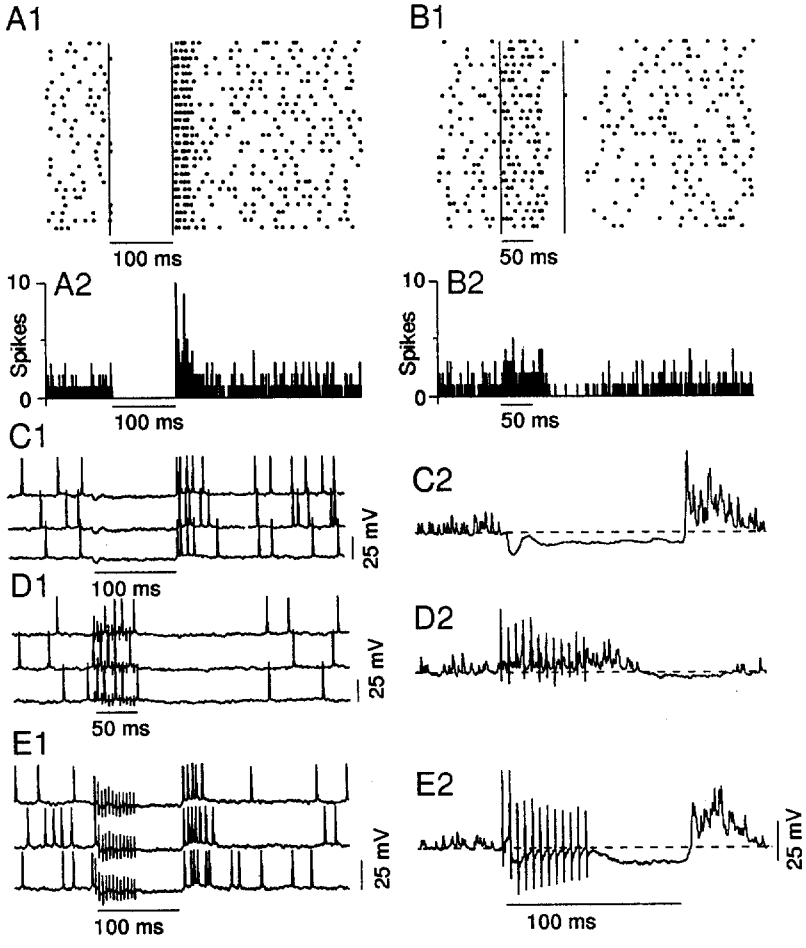

Fig. 12. A1,A2 Raster and PSTH displays of a nonbasilar pyramidal cell's responses to 0.375 mV/cm rms increases in EOD amplitude. **B1,B2** Responses of this same cell to 50 ms bursts of 50 μA, 50 μs pulses at a rate of 200 pulses/s delivered to a site that activated ovoid cell axons in the same manner as is shown in Fig. 10B. **C1** Three replicates of intracellularly recorded responses to the electrosensory stimulus of A1,A2. C2 A signal average of 15 replicates of responses to the electrosensory stimulus of C1. **D1,D2** Individual responses and a signal average of 15 replicates of responses to the electrical stimulation of ELL commissural fibers. **E1,E2** Individual responses and an average of 15 responses to the 100 ms electrosensory stimulus and 50 ms train of commissural fiber stimuli presented simultaneously. The voltage calibration of E2 holds for C2 and D2

the raster and PSTH displays of Fig. 12A1,A2. This cell responded to a 50 ms train of 50 μs commissure stimuli with increased firing as is shown in Fig. 12B1,B2. These data were recorded intracellularly and the responses to 3 replicates of the TRN electrosensory stimulus are shown in Fig. 12C1 along with an average of 15 replicates of this stimulus (Fig. 12C2). Nonbasilar pyramidal cells typically respond to increased receptor afferent activity with an initial sharp hyperpolarization followed by a somewhat smaller maintained hyperpolarization which in this case averaged about 7 mV. Figure 12D1,D2 shows the cell's responses to three presentations of the commissure stimulus and an average of 15 replicates. The commissure stimulus evokes spikes in this cell; the timing of these is variable relative to the individual stimulus pulses and a pause in firing occurs following the cessation of the stimulus. The average of Fig. 12D2 shows the development of about a 5 mV depolarization during the stimulus followed by a weak hyperpolarization which is sufficient to silence the cell. Three replicates of the cell's responses to simultaneous presentation of the 50 ms train of commissure stimuli and the 100 ms electrosensory stimulus are shown in Fig. 12E1. The hyperpolarization due to the electrosensory stimulus prevents the cell from firing in response to the commissure stimulus. The depolarization that results from the latter is more clearly seen superimposed on the hyperpolarization in the signal average (15 replicates) of Fig. 12E2.

The nonbasilar pyramidal cells are found in the most dorsal portion of the polymorphic cell layer and the ascending processes of the commissural axons do not enter this region, hence the NBP cells are not expected to be inhibited by these. The excitatory responses of the NBP cells are most likely a result of disinhibition. Nonbasilar pyramidal cell disinhibition is expected if commissural cells make inhibitory synaptic contact with the granule cells. The latter provide the principal inhibitory input to the NBP cells.

Discussion

The anatomical results of this study along with Maler and Mugnaini's (1986 and personal comm.) descriptions of GABAergic circuits within the electrosensory system of *Apteronotus* show that the ELL commissural connections are more complex than was previously thought. Both a rostral and caudal commissure exist, and the length of the former pathway plus the relatively small diameter of its constituent axons suggests that information carried via this route will be subject to a large conduction delay. Only polymorphic cells project via the rostral pathway and the length and small diameters of their axons may explain the earlier observation that only weak retrograde labeling of these cells occurred (Maler et al. 1982). The caudal pathway, on the other hand, seems specialized for rapid conduction and possibly the transmission of information about the timing of the electric organ discharges. The relatively short pathway, large axon diameter, gap junction transmission between receptor afferents and the ovoid cells (Maler et al. 1981; Yamamoto et al. 1989), and relatively strong phase coupling between the cells' firing and the EOD waveform support this conclusion.

Single cell labeling shows that individual ovoid cells project to both the ipsilateral and contralateral ELLs and that the axonal arborizations are restricted to within a single ELL segment. Ovoid cell terminal fields are very large, typically extending throughout the majority of the ELL's rostro-caudal extent. The ovoid cell soma fills labeled many dendritic fibers which ramified over long distances within the ELL deep fiber layer suggesting that ovoid cell receptive fields are also large. These extensive axonal arborizations indicate that single ovoid cells influence extensive regions of ELL circuitry bilaterally. Polymorphic axonal arborizations were not filled in this study, but Maler and Mugnaini (personal comm.) have recently shown, using *Phaseolus vulgaris* leucoagglutinin as a label, that polymorphic cells also project bilaterally. The rostro-caudal extent of their individual axonal arborizations remains to be determined.

The synaptic targets of polymorphic and ovoid cells are probably different. The terminal fields of polymorphic cells are restricted to the granule cell layer and contact granule cells and possibly other polymorphic cells (Maler et al. 1981). Ovoid cells almost certainly contact basilar pyramidal cells and deep basilar pyramidal cells since these are heavily invested with filled axon terminals following either HRP labeling of ovoid cells or GABA immunohistochemistry (Maler and Mugnaini 1986). Our results suggest that ovoid cells may also contact granule cells. Neither type of commissural neuron appears to contact the nonbasilar pyramidal cells. Our conclusions concerning potential synaptic targets are not definitive since they are based on light microscopic evidence. They are, however, largely in agreement with the results of an earlier Golgi-EM study of the synaptic organization of the ELL (Maler et al. 1981).

The responses of ovoid cells to stepwise changes in EOD amplitude show that they encode information about the transient phase of the stimulus as well as about the steady-state EOD amplitude. Both the high-frequency burst that characterizes these cells' responses to the transient phase of EOD increases as well as the steady firing frequency adopted during long-term changes in EOD amplitude are graded with stimulus strength (Fig. 6). There are also interesting differences in the magnitude and the time course of these responses depending on stimulus geometry. For a given stimulus amplitude, the transverse geometry always caused larger responses that adapted with longer time constants as compared to the mouth-tail stimuli. The differences in response magnitude contingent upon stimulus geometry must be interpreted cautiously, however, since it is not possible to insure that all regions of the body receive precisely the same stimulus intensities with different geometries. Local variations in stimulus amplitude contingent on stimulus geometry could possibly account for the differences in the magnitude of the responses shown in Fig. 6. Adaptation time constants also varied with stimulus geometry; being significantly shorter for the mouth-tail arrangement and this was independent of the stimulus amplitudes for which time constants could be accurately determined.

The more rapid adaptation of these neurons plus their weaker responses to symmetrical changes in EOD amplitude suggests that reciprocal inhibition among ovoid cells on opposite sides of the brain may occur.

Based upon the limited sample of polymorphic cells studied thus far, we conclude that at least a subset of these cells must receive their principal afferent input from ELL inhibitory interneurons rather than from electroreceptor afferents. They respond to ipsilateral increases in receptor afferent activity with decreased firing, their response latencies are long and comparable to those of nonbasilar pyramidal cells which are also driven by inhibitory interneurons, and, like the nonbasilar pyramidal cells, their resting activity is unrelated to the EOD waveform. The polymorphic cells differ from the nonbasilar pyramidal cells in that their resting firing frequency is higher and more regular, and their responses are very slowly adapting. The nonbasilar pyramidal cells adapt rapidly (Bastian 1981; Saunders and Bastian 1984; Shumway 1989).

The functional characteristics of these polymorphic cells differ from those expected based upon the anatomical description of their synaptic input. Maler et al. (1981) identified inhibitory interneurons (granule cells), polymorphic cells themselves, and receptor afferents as presynaptic elements. The former two are GABAergic cells and could produce the inhibitory responses seen in this study, but the receptor afferent inputs are expected to cause excitation. Perhaps the inhibitory inputs comprised the dominant inputs to the cells studied here. Our sample of polymorphic cells is very small and we cannot rule out the possibility that multiple physiological types of these cells exist which differ in their predominant synaptic input. Matsubara and Zhang (1992) have reported the presence of a wide variety of polymorphic neurons in the ELL of the related fish *Sternopygus*. Larger numbers of polymorphic cells need to be recorded from and morphologically identified in order to determine if they do form a heterogeneous population.

Responses to ELL commissure stimulation

We used direct electrical stimulation of the deep fiber layer of the contralateral ELL to activate commissural axons while recording from ELL pyramidal cells. We are certain that this technique activated ovoid cells since these were always monitored and orthodromic or antidromic activity was observed before and after pyramidal cells were studied. We cannot specify whether or not polymorphic cells were also activated. It is also possible that ascending efferents from the stimulated ELL were activated since these exit the ELL about 50 to 100 μm dorsal to the fibers that contribute to the caudal commissure. This latter possibility is less likely since moving the stimulation electrodes roughly 20 μm dorsal to an effective site of ovoid stimulation eliminated both ovoid cell antidromic spikes and the effects on pyramidal cell activity.

Rose (1989) observed that ELL pyramidal cells gave stronger responses to electrosensory stimuli presented with the transverse geometry as compared to similar stimuli presented with mouth-tail (symmetrical) geometry. Differences in responsiveness were noted for both basilar and nonbasilar pyramidal cells, and these results suggested that the symmetrical stimulus invoked a 'common mode rejection' mechanism that decreased pyramidal cell sensitivity to bilateral increases or decreases in receptor afferent activity.

The effects of electrical stimulation of commissural cell axons on pyramidal cells support this idea of common mode rejection. Activation of the commissural axons results in hyperpolarization of the basilar pyramidal cells, pauses in their resting activity, and attenuation of responses to simultaneously applied electrosensory stimuli (Fig. 11). These effects probably result from increased ovoid cell activity since these cells are the commissural source of GABAergic input to basilar pyramidal cells.

Nonbasilar pyramidal cells respond to commissural axon stimulation oppositely; they are depolarized and show enhanced firing frequency (Fig. 12). These effects are almost certainly the result of disinhibition. Polymorphic cells, and possibly ovoid cells, provide GABAergic input to the ELL granule cells. The granule cells provide the principal input to the NBP cells and this input is also inhibitory (Maler et al. 1981; Maler and Mugnaini 1986). Hence inhibition of granule cells resulting from commissural axon stimulation is expected to release the NBP cells from inhibition. The disinhibition of nonbasilar pyramidal cells resulting from electrical stimulation of the commissural axons could be due to either increased ovoid or polymorphic cell activity since both types are GABAergic and are probably presynaptic to granule cells. However, the NBP cells' reduced responsiveness to common mode electrosensory stimuli, as reported by Rose (1989), is unlikely to be mediated by polymorphic cells having the properties described above. Since these were inhibited by increased receptor afferent input their reduced activity would disinhibit the granule cells allowing them to respond more vigorously to increased afferent input. The result would be increased, not decreased, inhibitory responses of nonbasilar pyramidal cells. The reduced responsiveness of NBP cells to common mode electrosensory stimulation must be mediated by ovoid neurons or by another category of 'polymorphic cell' which is primarily driven by receptor afferents rather than by inhibitory interneurons.

Possible roles for commissural cells

Common mode rejection mechanisms have been more thoroughly studied in the dorsal nucleus of elasmobranchs. This structure is the first-order electrosensory processing region of non-teleost electroreceptive fish (Bullock 1982) and although these animals have only low-frequency (ampullary) electroreceptors the organization of the dorsal nucleus has many similarities to that of the ELL (Bodznick and Boord 1986). The extremely high sensitivity of the ampullary system results in significant changes in receptor afferent activity occurring in response to the animal's gill movements and possibly as a

result of other locomotor activities. The efferent neurons of the dorsal nucleus are, however, much less sensitive to these signals due to common mode rejection mechanisms involving both commissural cells and local interneurons with large receptive fields (Montgomery and Bodznick 1991; Montgomery 1984; New and Bodznick 1990; Bodznick and Montgomery 1993; Bodznick et al. 1993). Spatially extensive excitatory stimuli, or those having bilaterally symmetrical components, result in the dorsal nucleus efferent neurons receiving both excitatory receptor afferent input plus inhibitory inputs from interneurons or commissural cells which are also excited by the receptor afferents. These opposing inputs cancel. Spatially restricted stimuli preferentially activate the smaller excitatory receptive fields of the dorsal nucleus efferents which respond more vigorously in the absence of interneuronal or commissural inhibition.

The ovoid cells could be involved in a similar common mode rejection mechanism. The large bilateral axonal arborizations, probable large receptive fields, and the nonadapting responses make these cells well suited for conveying information about large-scale, long-term changes in the electrosensory environment to extensive portions of the ELL circuitry. Several situations can occur which result in spatially homogeneous changes in EOD amplitude that carry little useful information. Damage to the fragile tail and electric organ, changes in the animal's body geometry (tail bending), or changes in water conductivity (Knudsen 1975), can globally alter the electric organ discharge amplitude and, analogous to the situation in elasmobranchs, gill movements modulate the activity of tuberous electroreceptors that have receptive fields near the gills of *Apteronotus* (Bastian, unpublished observations). Rejection of these EOD alterations would be desirable.

The role of the ovoid cells in rejecting bilaterally symmetrical stimuli is summarized in the diagram of Fig. 13A. The direction of the arrows near synapses or cell bodies indicate the expected changes in a given cell's firing frequency (upward arrows, increased activity; downward, decreased firing) due to mouth-tail or transverse stimulus geometry. Receptor afferent activity is increased symmetrically by mouth-tail increases resulting in increased excitation of both ovoid and basilar pyramidal cells on both sides of the brain (Fig. 13A, filled and open arrows). The increased activity of the GABAergic ovoid cells is expected to reciprocally inhibit basilar pyramidal cells on both sides of the brain. These inhibitory inputs to the pyramidal cells' basilar dendrites are expected to partially cancel the excitatory effects of the increased receptor afferent activity thereby reducing the pyramidal cell responses as described by Rose (1989), and demonstrated by commissural axon stimulation (Fig. 11).

Transversely applied stimuli have the opposite effect on basilar pyramidal cells since they cause opposite signed changes in EOD amplitude on opposite sides of the body (Fig. 13B). In this case the depolarization of the basilar pyramidal cell due to increased receptor afferent activity (left side of Fig. 13B) is summed with reduced inhibitory drive (disinhibition, "d") due to reduced activity of the contralateral ovoid neuron resulting from decreased receptor afferent input on the right. Complimentary effects will occur for the basilar pyramidal cell on the right; its hyperpolarization due to reduced receptor afferent activity will be augmented by enhanced GABAergic input resulting from increased EOD amplitude on the left.

The ideas summarized in Fig. 13 not only suggest that the ovoid cells participate in the rejection of common mode signals, but also raise the possibility that the ovoid cells allow the ELLs to operate in a differential mode. Signals of opposite sign applied to opposite sides of the body evoke larger changes in pyramidal cell activity than would occur due to either signal presented alone (Fig. 13B). This latter capability is a consequence of the ovoid cells' high firing frequency in response to the normal EOD. Without the high resting frequency of ovoid cells significant pyramidal cell disinhibition resulting from reduced contralateral receptor afferent input would not be possible.

The ovoid neurons could also account for the differences in nonbasilar pyramidal cells' responses to mouth-tail and transversely applied stimuli if they provide inhibitory inputs to granule cells. Similar mechanisms for attenuation or heightened differential sensitivity can operate within a single ELL for signals that are spatially large or small, respectively, relative to the receptive fields of ovoid cells.

In addition to possible roles in rejecting longer-term common mode alterations in EOD amplitude, the short response latency, apparently high conduction velocity, and the strong phase relationship to the EOD waveform suggest a function in processing transients that occur in the electric organ discharge waveform. The amplitude

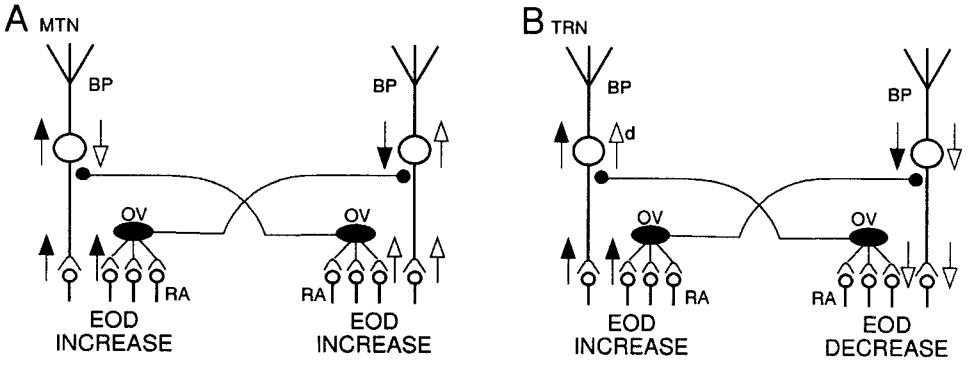

Fig. 13 A,B. Diagram illustrating bilateral projection of ovoid cells and the effects of their activity on basilar pyramidal cells. *Upward* and *downward arrows* symbolize increased and decreased firing frequency, respectively, and *filled* and *unfilled arrows* indicate effects originating on opposite sides of the body. Open synaptic terminals are excitatory and filled terminals are inhibitory. *BP*, basilar pyramidal cell; *d*, disinhibition; *OV*, ovoid cells; *RA*, receptor afferents

and frequency of the EOD of weakly electric fish can be modulated during a variety of social situations (Hagedorn 1986; Hopkins 1986; Heiligenberg 1986, 1991a,b; Kramer 1990 for reviews; Dye 1987; Metzner and Heiligenberg 1991; Heiligenberg et al. 1991; Zupanc and Maler 1993). In the case of *Apteronotus* a behavior known as a chirp, first described by Larimer and MacDonald (1968), seems to be a critical signal used in courtship and agonistic behaviors. This behavior consists of transient EOD accelerations typically accompanied by reduced EOD amplitude followed by a return to the normal EOD amplitude and frequency. Individual chirps last roughly 10 to 20 ms (Zupanc and Maler 1993) and are readily evoked by a conspecific's discharge or by a sinusoidal electric signal having a frequency within the species range.

Although the effects of chirps on the amplitude and time course of an individual's EOD can be complex as shown by Zupanc and Maler (1993), it is clear that a fish that produces a chirp will perceive an EOD modulation quite different from the EOD modulation due to a chirp received from another fish. The amplitude and frequency modulation resulting from the animal's own chirp will be similar in all regions of the body, hence it will have a strong common mode component. Chirps received from a conspecific will produce amplitude modulations and patterns of phase modulation of opposite sign in antipodal regions of the body. The sensitivity of the ovoid cells to transient changes in EOD amplitude may result in attenuation of the common mode EOD changes due to the animal's own chirp, while the enhanced sensitivity to differential signals predicted in conjunction with Fig. 13B may facilitate detection and identification of chirps generated by conspecifics distant from the receiver.

Possible roles of polymorphic cells in ELL electrosensory processing are less obvious. The polymorphic cells of *Apteronotus* and of the related fish *Sternopygus* are GABAergic (Maler and Mugnaini 1986, personal comm; Matsubara, personal comm.). Those that we have filled are inhibited by increased receptor afferent input indicating that their principal inputs are from granule cells, and their main synaptic targets are also the ELL granule cells. The role of polymorphic cells is further complicated by the fact that they possess apical dendrites which extend into the ELL molecular layers, hence they will be influenced by descending control systems. The polymorphic cells also project to the contralateral ELL via a very long pathway which must insert a significant conduction delay. Additional physiological studies are needed before reasonable hypotheses can be generated regarding the function of polymorphic cells. The anatomical segregation of polymorphic and ovoid cell axons into rostral and caudal commissures should allow the former to be manipulated separately. Electrical stimulation or local anesthetic application to the rostral commissure may provide additional clues as to the polymorphic cell function.

Acknowledgements. The authors are grateful to Drs. L. Maler, E. Mugnaini, and J. Matsubara for many helpful discussions and access to unpublished immunohistochemical studies of GABA distribution in weakly electric fish. Supported by NIH grant NS12337 to J.B., NSF graduate fellowship RCD 90–54797 to J. Courtright and NRSA DC00020-02 to J. Crawford.

References

Bastian J (1981) Electrolocation II: The effects of moving objects and other electrical stimuli on the activities of two categories of posterior lateral line lobe cells in *Apteronotus albifrons*. J Comp Physiol 144:481–494

Bastian J (1986a) Gain control in the electrosensory system mediated by descending inputs to the electrosensory lateral line lobe. J Neurosci 6:553–562

Bastian J (1986b) Gain control in the electrosensory system: a role for the descending projections to the electrosensory lateral line lobe. J Comp Physiol A158:505–515

Bastian J (1986c) Electrolocation: behavior, anatomy, and physiology In: Bullock TH, Heiligenberg W (eds) Electroreception. Springer, Berlin Heidelberg New York, pp 577–612

Bastian J (1993) The role of amino acid neurotransmitters in the descending control of electroreception. J Comp Physiol A172:409–423

Bastian J, Bratton B (1990) Descending control of electroreception. I. Properties of nucleus praeeminentialis neurons projecting indirectly to the electrosensory lateral line lobe. J Neurosci 10:1226–1240

Bastian J, Courtright J (1991) Morphological correlates of pyramidal cell adaptation rate in the electrosensory lateral line lobe of weakly electric fish. J Comp Physiol A168:393–407

Batschelet E (1981) Circular statistics in biology. Academic Press, London

Bodznick D, Boord RL (1986) Electroreception in Chondrichthyes. In: Bullock TH, Heiligenberg W (eds) Electroreception. Springer, Berlin Heidelberg New York, pp 225–256

Bodznick D, Montgomery JC (1993) Suppression of ventilatory reafference in the elasmobranch electrosensory system: Medullary neuron receptive fields support a common mode rejection mechanism. J Exp Biol 171:127–135

Bodznick D, Montgomery JC, Bradley DJ (1993) Suppression of common mode signals within the electrosensory system of the little skate *Raja erinacea*. J Exp Biol 171:107–125

Bratton B, Bastian J (1990) Descending control of electroreception. II. Properties of nucleus praeeminentialis neurons projecting directly to the electrosensory lateral line lobe. J Neurosci 10:1241–1253

Bullock TH (1982) Electroreception. Annu Rev Neurosci 5:121–170

Carr C, Maler L (1986) Electroreception in gymnotiform fish: central anatomy and physiology. In: Bullock TH, Heiligenberg W (eds) Electroreception. Springer, Berlin Heidelberg New York, pp 319–373

Dye J (1987) Dynamics and stimulus-dependence of pacemaker control during behavioral modulations in the weakly electric fish, *Apteronotus*. J Comp Physiol A161:175–185

Hagedorn M (1986) The ecology, courtship, and mating of gymnotiform electric fish. In: Bullock TH, Heiligenberg W (eds) Electroreception. Springer, Berlin Heidelberg New York, pp 497–525

Hagiwara S, Szabo T, Enger PS (1965) Electroreceptor mechanisms in a high-frequency weakly electric fish, *Sternarchus albifrons*. J Neurophysiol 28:784–799

Heiligenberg W (1986) Jamming avoidance responses. In: Bullock TH, Heiligenberg W (eds) Electroreception. Springer, Berlin Heidelberg New York, pp 613–649

Heiligenberg W (1991a) Sensory control of behavior in electric fish. Current Opinion in Neurobiol 1:633–637

Heiligenberg W (1991b) Neural nets in electric fish. MIT Press, Cambridge

Heiligenberg W, Dye J (1982) Labelling of electroreceptive afferents in a gymnotoid fish by intracellular injection of HRP: The mystery of multiple maps. J Comp Physiol 148:287–296

Heiligenberg W, Keller CH, Metzner W, Kawasaki M (1991) Structure and function of neurons in the complex of the nucleus

electrosensorius of the gymnotiform fish *Eigenmannia*: Detection and processing of electric signals in social communication. J Comp Physiol A169:151–164

Hopkins CD (1986) Behavior of Mormyridae. In: Bullock TH, Heiligenberg W (eds) Electroreception. Springer, Berlin Heidelberg New York, pp 497–525

Knudsen EI (1975) Spatial aspects of the electric fields generated by weakly electric fish. J Comp Physiol 99:103–118

Kramer B (1990) Electrocommunication in teleost fish. Springer, Berlin Heidelberg New York

Larimer JL, MacDonald JA (1968) Sensory feedback from electroreceptors to electromotor pacemaker centers in gymnotids. Am J Physiol 214:1253–1261

Maler L (1979) The posterior lateral line lobe of certain gymnotoid fish: quantitative light microscopy. J Comp Neurol 183:323–364

Maler L, Mugnaini E (1986) Immunohistochemical identification of GABAergic synapses in the electrosensory lateral line lobe of a weakly electric fish (*Apteronotus leptorhynchus*). Soc Neurosci Abstr 12:312

Maler L, Sas E, Carr CE, Matsubara J (1982) Efferent projections of the posterior lateral line lobe in gymnotiform fish. J Comp Neurol 211:154–164

Maler L, Sas E, Johnston S, Ellis W (1991) An atlas of the brain of the electric fish *Apteronotus leptorhynchus*. J Chem Neuroanat 4:1–38

Maler L, Sas E, Rogers J (1981) The cytology of the posterior lateral line lobe of high frequency electric fish (Gymnotidae): dendritic differentiation and synaptic specificity in a simple cortex. J Comp Neurol 158:87–141

Matsubara JA, Zhang J (1992) Local circuitry within the electrosensory lateral line lobe (ELLL) of *Sternopygus*: Role of polymorphic neurons. Soc Neurosci Abstr 18:348

Metzner W, Heiligenberg W (1991) The coding of signals in the electric communication of the gymnotiform fish *Eigenmannia*: From electroreceptors to neurons in the torus semicircularis of the midbrain. J Comp Physiol A169:135–150

Montgomery JC (1984) Noise cancellation in the electrosensory system of the thornback ray; common mode rejection of input produced by the animal's own ventilatory movement. J Comp Physiol A155:103–111

Montgomery J, Bodznick D (1991) Properties of medullary interneurons of the skate electrosense provide evidence for the neural circuitry mediating ventilatory noise suppression. Biol Bull 181:326

New JG, Bodznick D (1990) Medullary electrosensory processing in the little skate. II. Suppression of self-generated electrosensory interference during respiration. J Comp Physiol A167:295–307

Rose GJ (1989) Suppression of 'common mode' signals in the central electrosensory system. Soc Neurosci Abstr 15:348

Sas E, Maler L (1983) The nucleus praeeminentialis: a Golgi study of a feedback center in the electrosensory system of a gymnotid fish. J Comp Neurol 221:127–144

Sas E, Maler L (1987) The organization of afferent input to the caudal lobe of the cerebellum of the gymnotid fish *Apteronotus leptorhynchus*. Anat Embryol 177:55–79

Saunders J, Bastian J (1984) The physiology and morphology of two types of electrosensory neurons in the weakly electric fish *Apteronotus leptorhynchus*. J Comp Physiol A154:199–209

Shumway CA (1989) Multiple electrosensory maps in the medulla of weakly electric gymnotiform fish. I. Physiological differences. J Neurosci 9:4388–4399

Shumway C, Maler L (1989) GABAergic inhibition shapes temporal and spatial response properties of pyramidal cells in the electrosensory lateral line lobe of gymnotiform fish. J Comp Physiol A164:391–407

Szabo T, Fessard A (1974) Physiology of electroreceptors. In: Fessard A (ed) Handbook of sensory physiology III/3. Electroreceptors and other specialized receptors in lower vertebrates. Springer, Berlin Heidelberg New York, pp 59–124

Yamamoto T, Maler L, Hertzberg EL, Nagy JI (1989) Gap junction protein in weakly electric fish (Gymnotidae): Immunohistochemical localization with emphasis on structures of the electrosensory system. J Comp Neurol 289:509–536

Zupanc GKH, Maler L (1993) Evoked chirping in the weakly electric fish *Apteronotus leptorhynchus*: A biophysical analysis. J Exp Biol (in press)